NANO LETTERS

LETTER

pubs.acs.org/NanoLett

# Controlled Continuous Patterning of Polymeric Nanofibers on Three-Dimensional Substrates Using Low-Voltage Near-Field Electrospinning

Gobind S. Bisht,[†] Giulia Canton,[‡] Alireza Mirsepassi,[§] Lawrence Kulinsky,[§] Seajin Oh,[§,∥] Derek Dunn-Rankin,[§] and Marc J. Madou*[,†,‡,§,∥,⊥]

[†]Department of Biomedical Engineering, [‡]Department of Materials Science and Engineering, and [§]Department of Mechanical and Aerospace Engineering, University of California, Irvine, California 92617, United States

[∥]Ulsan National Institute of Science and Technology (UNIST), Banyeon-ri 100, Ulsan 689-798, Korea

[⊥]WCU (World Class University), National Research Foundation of Korea, Ministry of Education, Science and Technology, Korea

**ABSTRACT:** We report on a continuous method for controlled electrospinning of polymeric nanofibers on two-dimensional (2D) and three dimensional (3D) substrates using low voltage near-field electrospinning (LV NFES). The method overcomes some of the drawbacks in more conventional near-field electrospinning by using a superelastic polymer ink formulation. The viscoelastic nature of our polymer ink enables continuous electrospinning at a very low voltage of 200 V, almost an order of magnitude lower than conventional NFES, thereby reducing bending instabilities and increasing control of the resulting polymer jet. In one application, polymeric nanofibers are freely suspended between microstructures of 3D carbon on Si substrates to illustrate wiring together 3D components in any desired pattern.

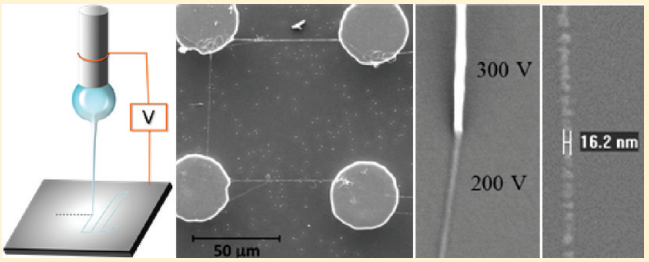


**KEYWORDS:** Electrospinning, polymeric nanofiber, micro/nanopatterning, suspended nanofibers, microfabrication, microelectromechanical systems (MEMS)

Fabrication of polymeric nanofibers has attracted considerable attention from researchers due to a wide variety of applications in the fields of sensors and actuators,[1−4] energy storage,[5,6] smart textiles,[7−10] optoelectronics,[11,12] tissue engineering,[13−16] prosthetics,[17] drug delivery,[18,19] microresonators,[20] and piezoelectric energy generators.[21] Several processes have been developed to tailor the properties of polymeric nanofibers to suit the particular needs of each application. These polymeric nanofiber modification techniques include chemical modification[22,23] surface deposition of metals,[24] functional doping,[25] and composite formation.[26−30] Polymeric nanofibers can also be pyrolyzed to yield thinner carbon nanofibers, opening up an even wider range of applications, including electrochemical sensors[31,32] and energy storage.[30,33,34] One of the key factors in the utilization of polymeric nanofibers in many of the aforementioned applications is the ability to accurately control the physical properties and positioning (patterning) of the produced nanofibers. One current method for precise patterning of polymeric nanofibers is through the use of electron-beam lithography (EBL) of resists.[35−37] However, EBL requires a laborious and lengthy process of e-beam cross-linking under high-vacuum conditions. Furthermore, high-vacuum equipment and sophisticated electronic lenses make the large scale use of EBL difficult and expensive. An alternative approach to precision patterning of polymeric nanofibers is based on the mechanical stretching of polymer droplets between three-dimensional (3D) microstructures using polymer-wetted probe tips.[38,39] This technique is similar to dip pen lithography (DPL)[40] and has an analogous drawback that neither technique can be operated continuously due to the frequent need for reinking the probe tip. Another option for continuous patterning of polymer nanofibers is far-field electrospinning (FFES), which is a well-known technique to produce polymeric nanofiber mats in large quantities.[41] However, FFES is hard to control due to the electric instabilities that are inherent to the electrospinning process.[28,42,43] Although work has been carried out to achieve alignment of nanofibers along a prescribed direction through the use of a rotating drum collector,[44−47] and by using electrical field manipulation,[28,48−50] precise 2D and 3D patterning is still very difficult to achieve with FFES. Recent efforts on a variant of electrospinning called near-field electrospinnning (NFES) produced some encouraging initial results, opening up a possibility of achieving scalable precision patterning with polymeric nanofibers. NFES offers the advantage of large scale manufacturability (inherent in electrospinning) combined with controlled electric field guidance (due to a reduced distance between the source and collector electrodes). However, the reported efforts[51] required the use of electric fields in excess of 200 kV/m for continuous NFES operation so that the resulting

**Received:** February 22, 2011
**Revised:** March 17, 2011
**Published:** March 29, 2011

**Table 1. Zero-Shear Viscosity and Relaxation Time Calculated for Different PEO Concentrations**

| | Zero-Shear Viscosity $\eta_o$ (Pa·s) | Relaxation Time $\lambda$ (s) |
|---|---|---|
| 1% PEO | 1.33 | 0.7 |
| 2% PEO | 28.70 | 10.0 |
| 3% PEO | 111.00 | 25.0 |

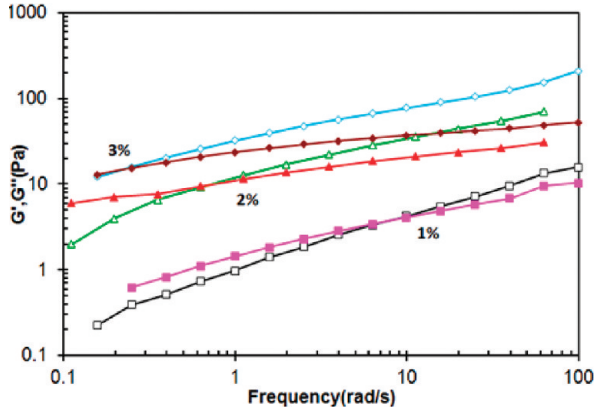


**Figure 1.** Elastic and viscous properties of PEO solution represented respectively by storage modulus ($G'$) [unfilled symbols] and loss modulus ($G''$) [filled symbols].

polymer jets still exhibit bending instabilities and thus limited control of polymeric nanofiber patterning.

Current state-of-the-art fabrication methods for polymeric nanofibers fail to deliver precise, inexpensive, fast, and continuous patterning capabilities. These deficiencies continue to hinder mass scale manufacturability and improvements in advanced applications of polymeric nanofibers. Patterning precision of nanofibers is often instrumental for better engineering of material properties in biological scaffolds[52] as well as for effective device operation such as in MEMS,[53] microelectronics,[54] and optoelectronics.[11,55]

In this Letter, we illustrate continuous electrospinning of polymeric nanofibers at low-voltage and low-electrical fields in a NFES-like setup. The key advance that allows for lowering of the voltage and attendant increase in patterning control of NFES is the use of a superelastic polymer ink. A superelastic polymer formulation can be stretched to enormous strains without breaking.[56,57] Solutions of such a polymer ink contain long entangled polymer chains that promote stretchability[58,59] and are expected to augment continuity of the electrospun jets. This facilitates the continuous electrospinning of the polymer jet into nanofibers.[60] Different concentrations of high molecular weight polyethylene oxide (MW = 4 000 000) from Dow Inc. (WSR-301) were tested as the superelastic polymer ink at 1, 2, and 3 wt % in deionized (DI) water. To obtain homogeneous PEO solutions, the mixtures were allowed to freely diffuse for 24 h followed by 96 h of vortex mixing in a single stirrer turbine at 30 rpm. Rheological properties of PEO were characterized by an Anton Paar rheometer and are tabulated in Table 1 and shown in Figure 1. The changes of the elastic modulus ($G'$) and the loss modulus ($G''$) of the polymer solution in a frequency sweep test are shown in Figure 1.

This graph reveals the elastic−solid versus dissipative−fluid-like behavior of a polymer solution. In the low frequency region,

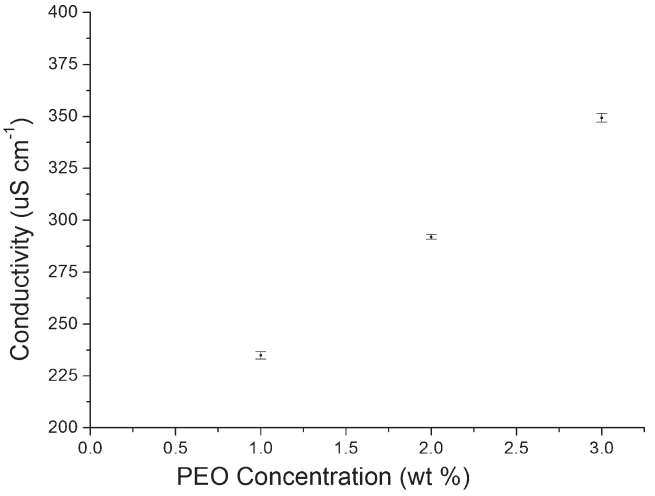


**Figure 2.** Conductivity vs PEO concentration (wt %) plot for the polymers tested for continuous NFES.

viscous behavior dominates ($G'' > G'$) due to relaxation of polymer chains and energy dissipation through the slippage of the polymer chains. At higher frequencies, the behavior changes to dominantly elastic ($G' > G''$) as polymer chains do not have time to slip past each other and the entanglement points act like fixed points for the polymer ink to store the energy in the network. The characteristic frequency at which $G' = G''$ is the reciprocal of the relaxation time of the polymeric ink. The crossover points of the $G'$ and $G''$ curves therefore reveal that increasing the PEO concentration increases the relaxation time of the polymer chains which indicates an increasing entanglement of the polymeric network. The conductivity of the polymer solutions was measured with an Oakton CON 510 conductivity probe equipped with a two-ring SS body conductivity electrode of cell constant $K = 1$. Figure 2 shows the conductivity versus PEO concentration graph that exhibits a rise in solution conductivity with the increase in PEO concentration (likely caused by impurities in the PEO powder).

The low-voltage NFES experiments use a 3 mL syringe bore fitted with a 27 gauge (~200 $\mu$m i.d.) type 304 stainless steel needle and mounted on a syringe pump (Harvard Apparatus, PHD 70-2001) to dispense the superelastic polymer ink at a feed rate lower than 1 $\mu$L/h. Pyrolyzed SU 8 carbon and Si were used as substrates; the voltage was applied to the needle, while the substrate was grounded. The substrate to needle distance was maintained at 1 mm. The voltage was turned on after the polymer formed a full-sized droplet of approximately 500 $\mu$m diameter at the needle tip, held in place by surface tension as seen in the schematic in Figure 3a and on the video-frames of Figure 5. The polymer jet does not self-initiate under the influence of the voltage because the electrostatic force cannot overcome the surface tension at the droplet−air interface. Therefore, the electrospinning process was initiated by introducing an artificial instability at the droplet−air interface with a glass microprobe tip (1 to 3 $\mu$m tip diameter) that resulted in a very high local electric field, sufficient to overcome the interfacial surface tension, giving rise to the formation of the Taylor cone and initiation of the polymer jet. The electrospinning phenomenon is illustrated in the schematic in Figure 3a, while Figure 3b shows a schematic of the electrospinning setup used to carry out the experiments.


dx.doi.org/10.1021/nl2006164 |*Nano Lett.* 2011, 11, 1831–1837

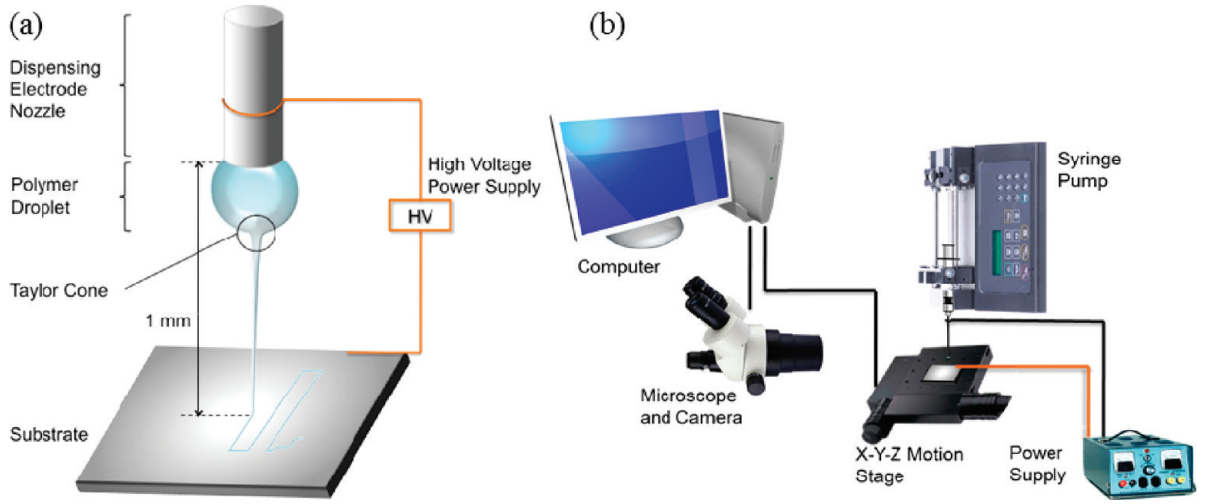


**Figure 3.** (a) A schematic of low-voltage NFES showing the polymer droplet, Taylor cone, and the polymer jet stretched by the electric field and patterned onto a substrate mounted on a movable stage. (b) The experimental setup used to carry out low-voltage NFES with a syringe pump, a micrometer resolution movable stage, and a power supply.

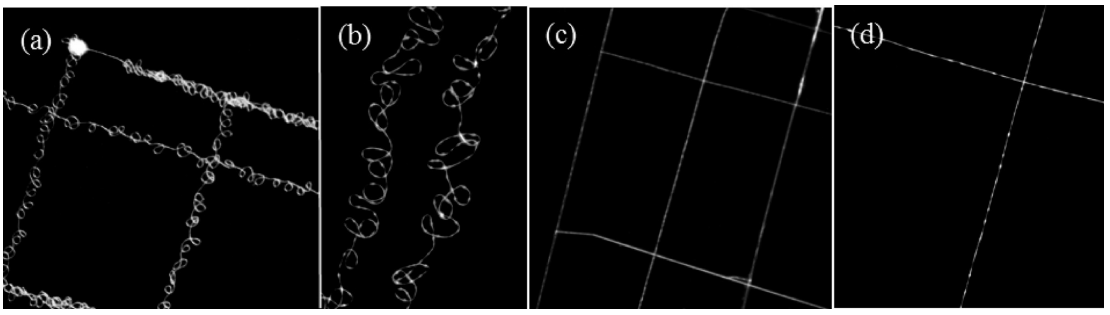


**Figure 4.** (a,b) Deposition pattern of nanofibers formed by high-voltage NFES of 2 wt % PEO at 600 V. The snakelike pattern is believed to occur due to high-speed oscillatory bending instability in the jet. (c,d) Deposition pattern of nanofibers formed by low-voltage NFES of 2 wt % PEO at 300 V. The straight aligned pattern is made possible perhaps by a combination of slower jetting and lower bending instability at a lower voltage. All deposition is done at 10−40 mm/s linear speed of the stage.

The patterning of nanofibers was carried out for up to 45 min to produce a stable continuous jet. Among the concentrations of PEO solutions that were tested, the use of 2 wt % PEO solution resulted in the most controlled continuous electrospinning. The lower concentration at 1 wt % PEO forms a very thin electrospinning jet that pinched off easily within a few seconds of initiation. Possible reasons for the latter are a faster loss of entanglement due to a lower relaxation time (Table 1) and a lower viscosity that reduces jet resistance to the bending instabilities, both causing easier breakage of the jet. On the other hand, the 3 wt % PEO solution forms a thicker jet due to its higher viscosity and higher conductivity, both of which are known to increase the effective polymer flow rate.[61,62] The 3 wt % PEO jet tends to harden before the onset of electrospinning and this hardening is likely caused by premature solvent evaporation during its longer flight in air due to an increased resistance to momentum change emanating from a higher viscosity. Therefore, we believe that 2 wt % PEO solution has the proper balance of viscosity, conductivity, and resistance to hardening that allows for low-voltage continuous electrospinning. The polymer jet was initiated at a higher voltage of 400−600 V to obtain a visible jet and after initiation the voltage was lowered to as low as 200 V with approximately 1 mm source to substrate operating distance.

This is a major improvement over conventional FFES methods that utilize voltages in excess of 10 kV at 10−15 cm operating distance[63] or even over recently reported NFES studies that used an initiation voltage of 1.5 kV and lowest operating voltage of 500 V at a 0.5 mm operating distance.[51,64] Our low-voltage NFES setup allows seamless electrospinning with superior control of nanofiber thickness and alignment. When the polymer jet is dispensed at 600 V, it produced looped fibers as seen in Figure 4a,b. This perturbation in the deposition pattern can be related to high speed oscillatory bending instability of the polymer jet caused by the electric field. At 300 V and lower, the perturbation phenomenon was eliminated and straight deposition patterns were obtained (as seen in Figure 4c,d). This could be achieved with slow stage speeds (20−40 mm/s) clearly demonstrating that the low-voltage NFES technique substantially reduces bending instabilities by operating at unprecedented low voltages made possible by the viscoelastic ink formulation. Previous reports on use of NFES for aligned patterning have required higher voltages combined with faster stage movement (120−1500 mm/s),[51,64] an obvious impediment to improving patterning precision.

Another advantage of lower voltage operation lies in reduction of the diameter of the jet, leading to thinner nanofibers. This is


dx.doi.org/10.1021/nl2006164 |*Nano Lett.* 2011, 11, 1831–1837

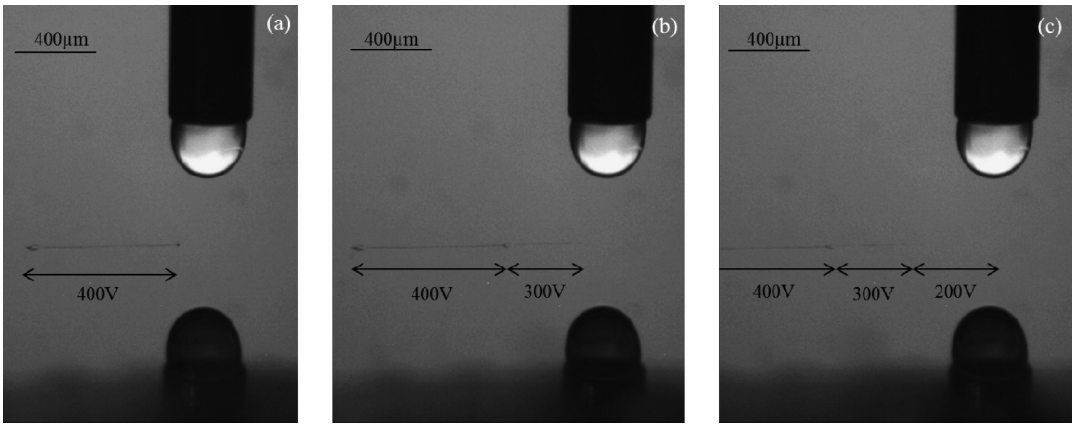


**Figure 5.** Low-voltage NFES in action at different voltages. The effect of voltage on nanofiber thickness can be seen in three consecutive frames from panels a to c when the voltage is switched from 400 to 200 V in steps of 100 V. The deposited nanofiber pattern can be seen due to scattering of projected light against the smooth Si surface. $X-Y$ stage speed is 40 mm/s.

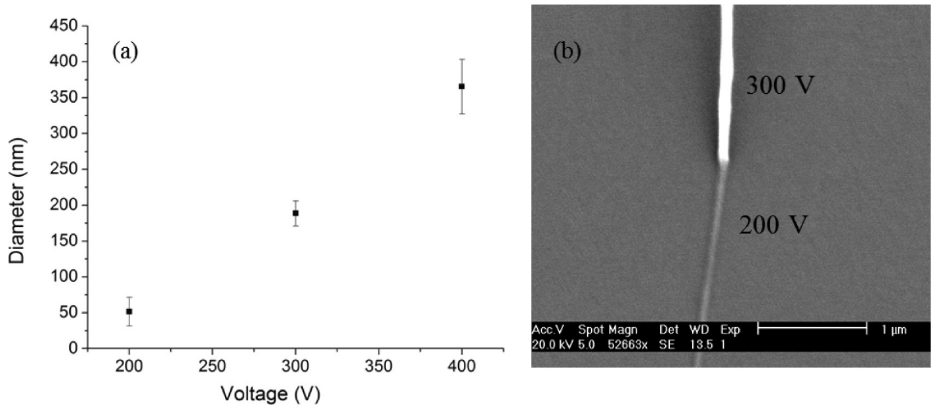


**Figure 6.** Correlation between nanofiber thickness and voltage applied between needle and substrate. (a) Diameter measurements of nanofibers electrospun at different voltages. (b) SEM image of a continuously electrospun nanofiber. The abrupt reduction of the nanofiber width corresponds to a voltage reduction step from 300 to 200 V.

most likely due to the lower electrostatic forces at play that reduce the feed rate of the polymer, thus reducing jet thickness. Therefore, the voltage can be manipulated to directly control the thickness of the nanofibers. Direct evidence of this relationship was observed in real time during electrospinning when a stepwise reduction in voltage reduced the thickness of the deposited nanofiber thus causing it to scatter less light making it difficult to observe, as the voltage was reduced (Figure 5). The deposited pattern went from a visible line at 400 V to almost invisible at 200 V under 60× magnification in the stereo microscope used to monitor the electrospinning process.

Further investigation into the effect of voltage on the thickness of nanofibers reveals an increasing linear trend of average diameter versus voltage as shown in Figure 6. This trend is opposite to that observed in far-field electrospinning where the fiber diameter decreases with higher applied voltage,[63−67] caused by the increase in the bending instability that further stretches the nanofibers.[68,69]

Very low voltage operation at 200 V allowed us to pattern unprecedentedly thin nanofibers in the range below 20 nm, the lowest thickness reported with NFES as seen in literature so far.[21,51,53] Such ultrathin nanofibers seem to be porous, perhaps an effect either due to beading of the nanofibers[58] or Pd/Au particle growth during sputtering (Figure 7). The fibers were sputtered with 6 nm Pd/Au layer to improve SEM resolution.

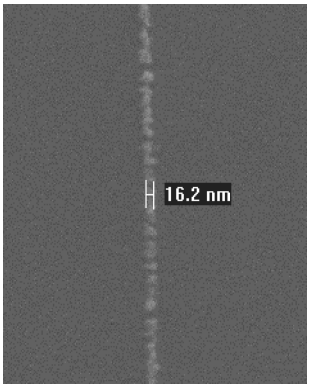


**Figure 7.** SEM picture of a nanofiber patterned directly with low-voltage NFES at 200 V.

All experiments were conducted on an automated $X-Y$ microstage (Prior Scientific Inc.) that is programmed to move the substrate in any desired pattern, for instance, in a perpendicular square wave pattern. Speed of the $X-Y$ stage has a


dx.doi.org/10.1021/nl2006164 |*Nano Lett.* 2011, 11, 1831–1837

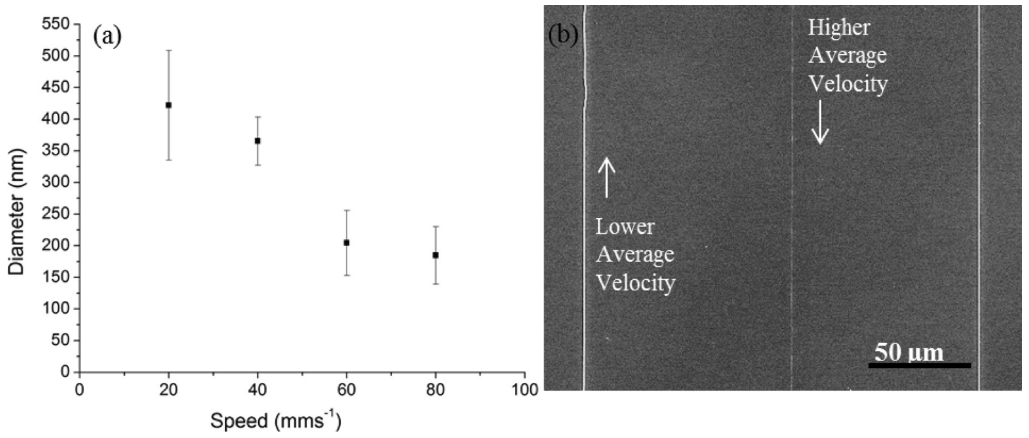


**Figure 8.** Correlation between nanofibers thickness and stage speed. The same pattern has been set for all the samples, while the maximum speed varies. Applied voltage: 400 V. (a) Diameter measurements of nanofibers electrospun at different stage maximum speeds. (b) SEM image of aligned nanofibers continuously electrospun according to the programmed pattern. Fiber thickness is shown to depend on the velocity of X-Y stage.

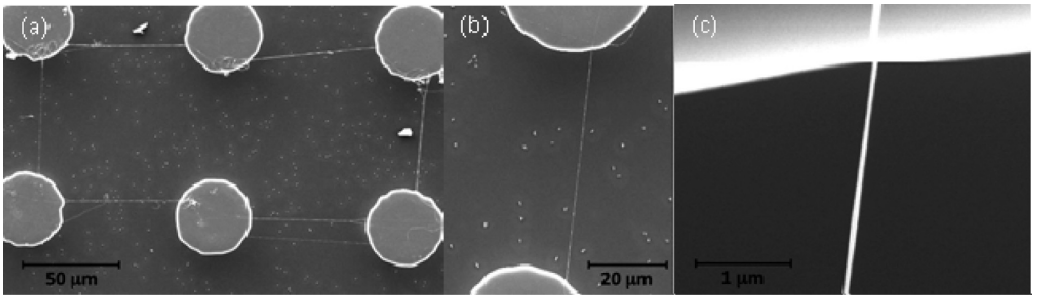


**Figure 9.** Suspended nanofiber on CMP arrays deposited by continuous NFES of viscoelastic 2 wt % PEO polymer at 300 V. (a) Six carbon posts connected to each other by nanofibers. (b) An individual nanofiber suspended between the posts (c) Close up of the suspended nanofiber.

significant effect on the physical characteristics of the deposited nanofibers as illustrated in Figure 8. As the stage accelerated to reach a certain speed, or decelerated to change direction, the diameter of the nanofiber was found to vary substantially. Lower average velocity leads to fiber thickening, and vice versa for a higher average velocity, most likely resulting from the mechanical stretching of the nanofibers between the point of contact on the substrate and the droplet (Figure 8b). While this effect can be avoided by patterning only in the constant velocity regime, it is also feasible to use the stage motion to create a smooth continuous transition between nanofibers of different thickness.

We further demonstrate the ability to integrate low-voltage NFES "writing" capability with 3D substrates by suspending nanofibers on carbon micropost arrays on a Si substrate. In a typical example, we use posts of a height of 40 $\mu$m, a diameter of 30 $\mu$m, an interpostal distance of 100 $\mu$m. These carbon post arrays are fabricated by the pyrolysis of high-aspect ratio SU-8 structures in a reducing environment. Details about the fabrication process of carbon MEMS arrays can be found in publications on carbon MEMS.[70,71] The writing of suspended polymeric nanofibers between carbon posts in an array was successfully carried out at a voltage of 200 V. The nanofiber deposition was monitored in situ through a stereo microscope. SEM pictures in Figure 9 show that both individual and multiple nanofibers were directly suspended between the posts. These nanofibers can be coated with metal to function as connectors and sensing elements on 3D microstructures. In the latter case, the sensing elements will exhibit higher signal-to-noise ratio compared to flat electrode geometries, resulting in enhanced sensitivity for chemical and biological sensors. Pyrolysis of these polymeric nanofibers into carbon will also enable conductive behavior with additional shrinkage of dimension[71] and versatile functionalization chemistry.[72−74]

In this study, we have demonstrated the ability to continuously pattern nanofibers on 2D and 3D substrates. This was made possible with the right balance of viscosity and elasticity of the polymer ink formulation that enables electrospinning at very low voltages. The low-voltage regime allows for a better control of patterning perturbations caused by bending instabilities ordinarily dominant in higher voltage ranges of conventional NFES and far-field electrospinning. Thickness control of patterned nanofibers is conveniently effected through applied voltage and/or stage speed manipulation to deposit ultrathin nanofibers. This fabrication ability will permit the use of electrospun nanofiber based wiring of structural and functional components in MEMS, microelectronics, and sensor devices. We believe that other applications can also include customized patterning of specialized polymeric nanofibers for production of advanced fabrics[75] and improved biomimicry for scaffolds[76] in tissue engineering.

## AUTHOR INFORMATION

### Corresponding Author

*E-mail: mmadou@uci.edu. Phone: 19498246585.

## ■ ACKNOWLEDGMENT

The authors are grateful to Dr. Horacio Kido, Rotaprep, Inc., and Mr. Sergiy Nesterenko for their support in use and control of XY Microstage, Mr. Jefferey Catterlin for technical support, Mina Rohani for jet dynamics guidance, and Integrated Nanosystems Research Facility (INRF) at University of California, Irvine for the use of microfabrication equipment and resources. This research was supported by the National Science Foundation Grant NIRT-0709085 and by UC Lab Fees Award 09-LR-09-117362 and WCU (World Class University) program (R32-2008-000-20054-0) through the National Research Foundation of Korea funded by the Ministry of Education, Science, and Technology.

## ■ REFERENCES

(1) Liu, H.; Kameoka, J.; Czaplewski, D.; Craighead, H. *Nano Lett.* **2004**, *4*, 671.
(2) Hahm, J.; Lieber, C. M. *Nano Lett.* **2004**, *4*, 51.
(3) Kameoka, J.; Verbridge, S. S.; Liu, H.; Czaplewski, D. A.; Craighead, H. G. *Nano Lett.* **2004**, *4*, 2105.
(4) Wang, M. C. P.; Gates, B. D. *Mater. Today* **2009**, *12*, 34.
(5) Yun, K.; Cho, B.; Jo, S.; Lee, W.; Cho, W.; Park, K.; Kim, H.; Kim, U.; Ko, S.; Chun, S. WO Patent WO/2001/089,023, 2001.
(6) Choi, S. W.; Jo, S. M.; Lee, W. S.; Kim, Y. R. *Adv. Mater.* **2003**, *15*, 2027.
(7) Ro ek, Z.; Kaczorowski, W.; Lukáš, D.; Louda, P.; Mitura, S. *J. Achiev. Mater. Manuf. Eng.* **2008**, *27*, 35.
(8) Pant, H.; Bajgai, M.; Nam, K.; Seo, Y.; Pandeya, D.; Hong, S.; Kim, H. *J. Hazard Mater.* **2010**, *185*, 7.
(9) Lee, S.; Obendorf, S. *Text. Res. J.* **2007**, *77*, 696.
(10) Gibson, P.; Schreuder-Gibson, H.; Rivin, D. *Colloids Surf., A* **2001**, *187*−*188*, 469.
(11) Di Benedetto, F.; Camposeo, A.; Pagliara, S.; Mele, E.; Persano, L.; Stabile, R.; Cingolani, R.; Pisignano, D. *Nat. Nanotechnol.* **2008**, *3*, 614.
(12) Pagliara, S.; Camposeo, A.; Cingolani, R.; Pisignano, D. *Appl. Phys. Lett.* **2009**, *95*, 263301.
(13) Jin, H.-J.; Chen, J.; Karageorgiou, V.; Altman, G. H.; Kaplan, D. L. *Biomaterials* **2004**, *25*, 1039.
(14) Mo, X. M.; Xu, C. Y.; Kotaki, M.; Ramakrishna, S. *Biomaterials* **2004**, *25*, 1883.
(15) Yoshimoto, H.; Shin, Y. M.; Terai, H.; Vacanti, J. P. *Biomaterials* **2003**, *24*, 2077.
(16) Li, W.-J.; Laurencin, C. T.; Caterson, E. J.; Tuan, R. S.; Ko, F. K. *J. Biomed. Mater. Res.* **2002**, *60*, 613.
(17) Nguyen Vu, T.; Chen, H.; Cassell, A.; Andrews, R.; Meyyappan, M.; Li, J. *Small* **2006**, *2*, 89.
(18) Luu, Y.; Kim, K.; Hsiao, B.; Chu, B.; Hadjiargyrou, M. *J. Controlled Release* **2003**, *89*, 341.
(19) Zeng, J.; Xu, X.; Chen, X.; Liang, Q.; Bian, X.; Yang, L.; Jing, X. *J. Controlled Release* **2003**, *92*, 227.
(20) Zande, A. M. v. d.; Barton, R. A.; Alden, J. S.; Ruiz-Vargas, C. S.; Whitney, W. S.; Pham, P. H. Q.; Park, J.; Parpia, J. M.; Craighead, H. G.; McEuen, P. L. *Nano Lett.* **2010**, *10*, 4869.
(21) Chang, C.; Tran, V. H.; Wang, J.; Fuh, Y.-K.; Lin, L. *Nano Lett.* **2010**, *10*, 726.
(22) Agarwal, S.; Wendorff, J. H.; Greiner, A. *Macromol. Rapid Commun.* **2010**, *31*, 1317.
(23) Reneker, D. H.; Yarin, A. L. *Polymer* **2008**, *49*, 2387.
(24) Pinto, N.; Carrion, P.; Quinones, J. *Mater. Sci. Eng., A* **2004**, *366*, 1.
(25) Huang, K.; Wan, M.; Long, Y.; Chen, Z.; Wei, Y. *Synth. Met.* **2005**, *155*, 495.
(26) Wang, X.; Kim, Y.-G.; Drew, C.; Ku, B.-C.; Kumar, J.; Samuelson, L. A. *Nano Lett.* **2004**, *4*, 331.
(27) Huang, J.; Wang, D.; Hou, H.; You, T. *Adv. Funct. Mater.* **2008**, *18*, 441.
(28) Li, D.; Wang, Y.; Xia, Y. *Nano Lett.* **2003**, *3*, 1167.
(29) Hou, H.; Reneker, D. *Adv. Mater.* **2004**, *16*, 69.
(30) Wang, L.; Yu, Y.; Chen, P.; Zhang, D.; Chen, C. *J. Power Sources* **2008**, *183*, 717.
(31) Vamvakaki, V.; Tsagaraki, K.; Chaniotakis, N. *Anal. Chem.* **2006**, *78*, 5538.
(32) Jang, J.; Bae, J. *Sens. Actuators, B* **2007**, *122*, 7.
(33) Kim, C.; Yang, K.; Kojima, M.; Yoshida, K.; Kim, Y.; Kim, Y.; Endo, M. *Adv. Funct. Mater.* **2006**, *16*, 2393.
(34) Yoon, S.; Park, C.; Yang, H.; Korai, Y.; Mochida, I.; Baker, R.; Rodriguez, N. *Carbon* **2004**, *42*, 21.
(35) Malladi, K.; Wang, C.; Madou, M. *Carbon* **2006**, *44*, 2602.
(36) Zou, Z.; Kai, J.; Ahn, C. *J. Micromech. Microeng.* **2009**, *19*, 055002.
(37) Kim, G.-T.; Gu, G.; Waizmann, U.; Roth, S. *Appl. Phys. Lett.* **2002**, *80*, 1815.
(38) Harfenist, S.; Cambron, S.; Nelson, E.; Berry, S.; Isham, A.; Crain, M.; Walsh, K.; Keynton, R.; Cohn, R. *Nano Lett.* **2004**, *4*, 1931.
(39) Nain, A.; Amon, C.; Sitti, M. *IEEE* **2004**, 224.
(40) Jiang, H.; Stupp, S. I. *Langmuir* **2005**, *21*, 5242.
(41) Reneker, D. H.; Yarin, A. L.; Zussman, E.; Xu, H. In *Advances in Applied Mechanics*; Hassan, A., Erik van der, G., Eds.; Elsevier: New York, 2007; Vol. 41, p 43.
(42) Doshi, J.; Reneker, D. *J. Electrost.* **1995**, *35*, 151.
(43) Yu, J.; Rutledge, G. In *Encyclopedia of Polymer Science and Technology*; Mark, H. F., Ed.; John Wiley & Sons: New York, 2007.
(44) Matthews, J. A.; Wnek, G. E.; Simpson, D. G.; Bowlin, G. L. *Biomacromolecules* **2002**, *3*, 232.
(45) Katta, P.; Alessandro, M.; Ramsier, R. D.; Chase, G. G. *Nano Lett.* **2004**, *4*, 2215.
(46) Kim, K.; Lee, K.; Khil, M.; Ho, Y.; Kim, H. *Fiber Polym.* **2004**, *5*, 122.
(47) Wannatong, L.; Sirivat, A.; Supaphol, P. *Polym. Int.* **2004**, *53*, 1851.
(48) Teo, W.; Ramakrishna, S. *Nanotechnology* **2005**, *16*, 1878.
(49) Theron, A.; Zussman, E.; Yarin, A. *Nanotechnology* **2001**, *12*, 384.
(50) Kessick, R.; Fenn, J.; Tepper, G. *Polymer* **2004**, *45*, 2981.
(51) Chang, C.; Limkrailassiri, K.; Lin, L. *Appl. Phys. Lett.* **2008**, *93*, 123111.
(52) Lee, C. H.; Shin, H. J.; Cho, I. H.; Kang, Y.-M.; Kim, I. A.; Park, K.-D.; Shin, J.-W. *Biomaterials* **2005**, *26*, 1261.
(53) Zheng, G.; Li, W.; Wang, X.; Wu, D.; Sun, D.; Lin, L. *J. Phys. D: Appl. Phys.* **2010**, *43*, 415501.
(54) Zheng, G.; Dai, Y.; Wang, L.; Sun, D. Proceedings of IEEE-Nano 2207, Hong Kong, People's Republic of China, August 2−5, 2007; IEEE: New York, 2007; pp 791−794; doi: 10.1109/NANO.2007.4601304.
(55) Hellmann, C.; Belardi, J.; Dersch, R.; Greiner, A.; Wendorff, J.; Bahnmueller, S. *Polymer* **2009**, *50*, 1197.
(56) Obukhov, S. P.; Rubinstein, M.; Colby, R. H. *Macromolecules* **1994**, *27*, 3191.
(57) Isaev, A. I.; Berezhnaya, G. V.; Malkin, A. Y. *J. Eng. Phys. Thermophys.* **1973**, *24*, 69.
(58) Fong, H.; Chun, I.; Reneker, D. H. *Polymer* **1999**, *40*, 4585.
(59) Shenoy, S. L.; Bates, W. D.; Frisch, H. L.; Wnek, G. E. *Polymer* **2005**, *46*, 3372.
(60) Feng, J. J. *J. Non-Newtonian Fluid Mech.* **2003**, *116*, 55.
(61) Reneker, D.; Yarin, A.; Fong, H.; Koombhongse, S. *J. Appl. Phys.* **2000**, *87*, 4531.
(62) Heikkilä, P.; Harlin, A. *Express Polym. Lett.* **2009**, *3*, 9.
(63) Ramakrishna, S. *An introduction to electrospinning and nanofibers*; World Scientific Pub. Co. Inc.: New York, 2005.
(64) Sun, D.; Chang, C.; Li, S.; Lin, L. *Nano Lett* **2006**, *6*, 839.
(65) Jalili, R.; Morshed, M.; Ravandi, S. A. H. *J. Appl. Polym. Sci.* **2006**, *101*, 4350.
(66) Lee, J. S.; Choi, K. H.; Ghim, H. D.; Kim, S. S.; Chun, D. H.; Kim, H. Y.; Lyoo, W. S. *J. Appl. Polym. Sci.* **2004**, *93*, 1638.

(67) Megelski, S.; Stephens, J. S.; Chase, D. B.; Rabolt, J. F. *Macromolecules* **2002**, *35*, 8456.
(68) Fridrikh, S. V.; Yu, J. H.; Brenner, M. P.; Rutledge, G. C. *Phys. Rev. Lett.* **2003**, *90*, 144502.
(69) Shin, Y.; Hohman, M.; Brenner, M.; Rutledge, G. *Appl. Phys. Lett.* **2001**, *78*, 1149.
(70) Wang, C.; Jia, G.; Taherabadi, L.; Madou, M. *J. Microelectromech. Syst.* **2005**, *14*, 348.
(71) Park, B. Y.; Taherabadi, L.; Wang, C.; Zoval, J.; Madou, M. J. *J. Electrochem. Soc.* **2005**, *152*, J136.
(72) Liu, J.; Cheng, L.; Liu, B.; Dong, S. *Langmuir* **2000**, *16*, 7471.
(73) Marwan, J.; Addou, T.; Bélanger, D. *Chem. Mater.* **2005**, *17*, 2395.
(74) Liu, J.; Dong, S. *Electrochem. Commun.* **2000**, *2*, 707.
(75) Chen, L.; Bromberg, L.; Lee, J. A.; Zhang, H.; Schreuder-Gibson, H.; Gibson, P.; Walker, J.; Hammond, P. T.; Hatton, T. A.; Rutledge, G. C. *Chem. Mater.* **2010**, *22*, 1429.
(76) Lowery, J. L.; Datta, N.; Rutledge, G. C. *Biomaterials* **2010**, *31*, 491.